Space-time correlations of the transverse velocity fluctuation in pipe flow

J. Sabot, J. Renault, and G. Comte-Bellot

Laboratoire de Mécanique des Fluides, Ecole Centrale de Lyon, 69130 Ecully, France

(Received 20 January 1973)

Memory times are smaller for transverse velocity components than for longitudinal components. For the former less downstream–upstream asymmetries are apparent in the optimal space–time isocorrelation contours.

Because of its homogeneity in the downstream direction, a fully developed turbulent pipe flow allows large longitudinal separations, and hence large time delays, for investigation of space-time correlations. For the two-point, two-time double correlation coefficients defined as

$$R_{ij}(\mathbf{x}; r_1, r_2, r_3; \tau) \equiv \frac{\overline{u_i(\mathbf{x}, t)u_j(\mathbf{x}+\mathbf{r}, t+\tau)}}{[\overline{u_i^2(\mathbf{x}, t)}]^{1/2}\cdot[\overline{u_j^2(\mathbf{x}+\mathbf{r}, t)}]^{1/2}}$$

an extensive survey has already been carried out in the case of the longitudinal (streamwise) velocity components.[1–3] Measurements were made for $\mathbf{x}$ located at various distances from the wall of a circular duct and for $\mathbf{r}$ lying in the regions $r_1 \gtrless 0$, $r_2 \gtrless 0$, and $r_3 = 0$. The results concerned either the pure spatial autocorrelation relative to $\tau = 0$, or the optimal space-time autocorrelation, defined as the maximum reached by R_{ij}, for any given $\mathbf{r}$, at a certain time delay $\tau = \tau_M$. In this latter group, special attention was paid to the optimal space-time correlations corresponding to $r_1 \neq 0$, $r_2 = r_3 = 0$, because they can be considered as pure time autocorrelations in a frame traveling at the convection speed $U_c \equiv r_1/\tau_M$. For example, in nearly isotropic grid-generated turbulence, full and narrow-band velocity signals were measured and analyzed.[4] For pipe flow, the scaling factor for the time correlations was found to be of the order of $L_{11}^{(1)}/u_1'$ (except in the central region); $L_{11}^{(1)}$ is the integral length (in the streamwise direction) of the streamwise turbulent velocity component, and u_1' is the rms value of that component.[2] This scale also seems to fit other flows, for instance, the inner region of boundary layers[5] and the experimental representation of homogeneous turbulent shear flow.[6] Asymmetries of the complete optimal space-time isocorrelation contours were also presented[3] ($r_1, r_2 \gtrless 0$), thus extending the measurements made by Favre *et al.*[7] in boundary layers.

The present field of research deals with the transverse (normal to the wall) turbulent velocity component. The autocorrelation of this transverse component is investigated, together with the two possible cross correlations of streamwise and transverse components, which depend on the component selected at point $\mathbf{x}$. Preliminary results of this systematic research are presented, for one Reynolds number and a single fixed distance from the wall. To date, little work has been done on this subject. Available results deal with a boundary layer[8] and with a nearly homogeneous turbulent shear flow.[9]

The experiments reported here are performed in a smooth circular pipe of diameter $D = 2R = 10$ cm. The Reynolds number based on D and on the pipe axis velocity is $\mathrm{Re} = 1.35 \times 10^5$. The fixed probe is at $x_1 = 95D$ from the pipe inlet, and at $x_2/R = 0.50$ from the wall. At this location, the mean velocity gradient $\partial U_1/\partial x_2$ is 95 sec^{-1}, with $\bar{U}_1 \approx 18.5$ m/sec; the rms values of the longitudinal and transverse turbulent velocity components are $u_1' = 1.45u^*$ and $u_2' = 0.88u^*$, with $u^* = 0.78$ m/sec; the shear stress is $\overline{u_1u_2}/u_1'u_2' = -0.40$. For the separation vector $\mathbf{r}$ locating the mobile probe with respect to the fixed probe, $r_1 > 0$ indicates a downstream separation, and $r_2 > 0$ a transverse separation away from the wall. The azimuthal separation r_3 is always zero.

The hot-wire probes used are miniature DISA types: 55 F 14, 55 F 11, and 55 A 38. They are fed by DISA constant-temperature anemometers model 55 D 01 without linearizing circuit. The downstream probe is a conventional X-wire, from which the u_1 and u_2 components are separated by means of operational amplifiers (Burr Brown type 3003/15). The upstream probe is a single hot-wire in order to reduce the aerodynamic disturbances. It is normal to the mean flow for measurements of R_{12} and control tests of R_{11}, and successively inclined at $+45°$ and $-45°$ for measurements of R_{21} and R_{22}. In the latter case correlations R_{2i} (with $i = 1$ or 2) are obtained by means of

$$R_{2i} = \frac{\overline{[u_1+u_2](x_1, t)u_i(x_1+r_1, t+\tau) - [u_1-u_2](x_1, t)u_i(x_1+r_1, t+\tau)}}{2[\overline{u_2^2}]^{1/2}[\overline{u_i^2}]^{1/2}}$$

All the time correlations are set up by a real-time correlator (Soc. Appl. Ind. Physique type CTR 100 or Hewlett–Packard model 3721 A). The frequency bandwidth is in the range 4 Hz–20 KHz.

One of the main characteristics of the optimal space-time correlations is the initial optimal time delay $\tau_M^*(r_2)$, where the maximum of $R_{ij}(\mathbf{x}; r_1, r_2, 0; \tau)$ occurs when $r_1 = 0$. For R_{11} a delay clearly different

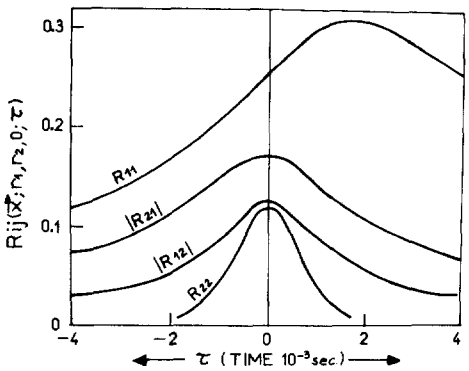

FIG. 1. Space-time correlation functions $R_{ij}(\mathbf{x}; r_1, r_2, 0; \tau)$ vs τ for $i, j=1$ or 2; $x_2/R=0.50$; $r_1/R=0$, $r_2/R=-0.30$.

from zero has been obtained, approximately related—using the Taylor hypothesis—to the asymmetry in r_1 of the pure spatial isocorrelation contours.[3] Here, for R_{22}, R_{12}, and R_{21}, Fig. 1 shows that $\tau_M{}^*$ is approximately zero and Fig. 2 shows that the pure spatial correlations are symmetric in r_1. At larger r_1, and for $r_2=0$, we have also verified that the R_{22}, $|R_{12}|$, and $|R_{21}|$ space-time correlations reach their maximal values together at about the same time delay; hence, the convection velocity U_c does not depend significantly on the correlation investigated.

Complete optimal isocorrelation contours are given in Fig. 3. The R_{22}, R_{12}, and R_{21} contours have zero slopes at $r_1=0$, in contrast with those of R_{11}. This follows from the previous results ($\tau_M{}^*\approx 0$ and symmetry in r_1 of the pure spatial correlations). These contours, in particular, the R_{22} contours, extend less in the r_1 and r_2 directions than those of R_{11}.

The time correlations of R_{22}, R_{12}, and R_{21} in the convected frame are given in Fig. 4 along with the time correlation of R_{11} obtained[2] previously. At small time delays, about $\tau_M \lesssim 25\times 10^{-3}$ sec in the present investigation, $|R_{12}|$ or $|R_{21}|$ decay more slowly than R_{22} or R_{11} as was also noted in the uniform shear flow measurements of Harris and Corrsin.[9] This result seems due to the fact that the small-scale turbulent structures,

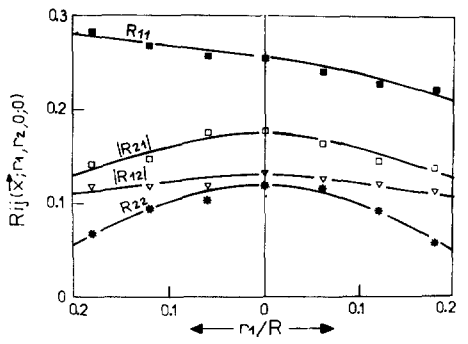

FIG. 2. Streamwise spatial correlation functions $R_{ij}(\mathbf{x}; r_1, r_2, 0; 0)$ for $i, j=1$ or 2; $x_2/R=0.50$; $r_2/R=-0.30$.

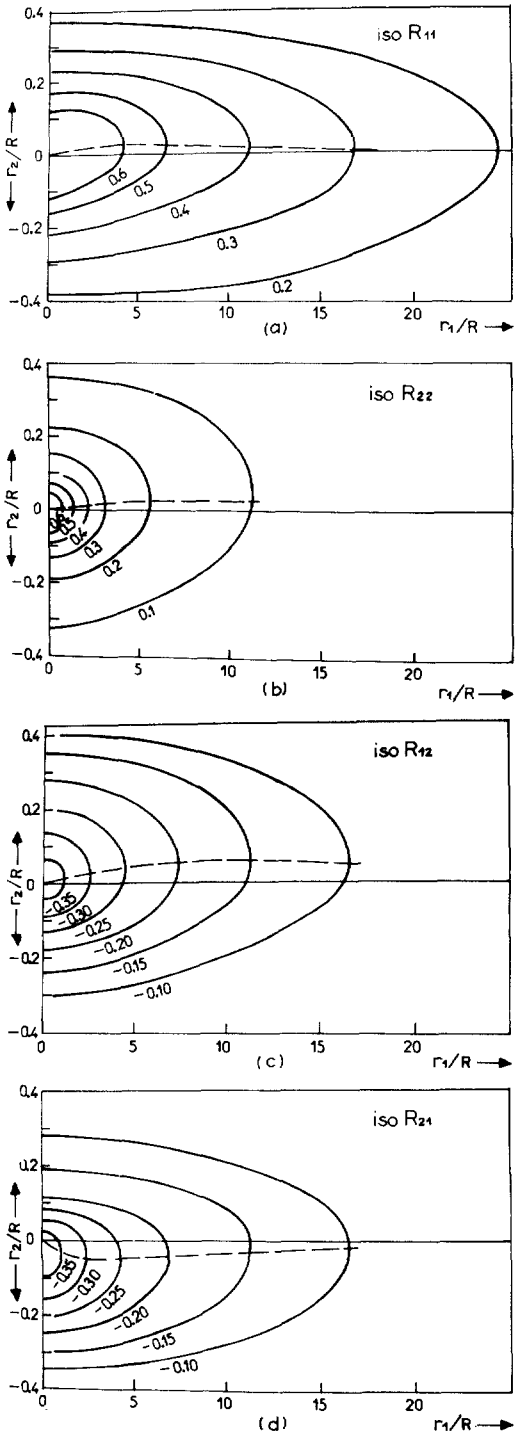

FIG. 3. Space-time isocorrelation contours $[R_{ij}(\mathbf{x}; r_1, r_2, 0; \tau_M) = \text{Const.}]$ for optimum time delay; $i, j=1$ or 2; $x_2/R=0.50$.

which mostly affect the initial decay of the time correlations, contribute less to $|R_{12}|$ or $|R_{21}|$ than to R_{22} or R_{11}. This behavior is modified at higher time delays: R_{11} exhibits the slowest decay, and R_{22} the fastest, as was also observed in the inner part of a boundary layer by Blackwelder and Kovasznay.[8]

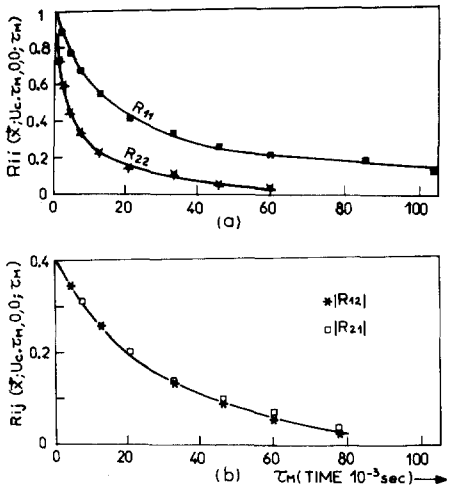

FIG. 4. Time correlation functions in convected frame; $x_2/R=0.50$.

Integral time scales can be deduced from the correlation curves of Fig. 4. We define them as

$$\Theta_{ij} \equiv \frac{[\overline{u_i^2}(\mathbf{x}, t)]^{1/2}[\overline{u_j^2}(\mathbf{x}, t)]^{1/2}}{\overline{u_i u_j}(\mathbf{x}, t)} \times \int_0^\infty R_{ij}(\mathbf{x}; U_c\tau_M, 0, 0; \tau_M)\, d\tau_M$$

to obtain the effective times characterizing the coherence loss. For the present investigation, these times are

$$\Theta_{11} \approx 48 \times 10^{-3} \text{ sec},$$

$$\Theta_{12} \approx \Theta_{21} \approx 29 \times 10^{-3} \text{ sec},$$

$$\Theta_{22} \approx 10 \times 10^{-3} \text{ sec}.$$

On the other hand,

$$L_{11}^{(1)}/u_1' \approx 44 \times 10^{-3} \text{ sec}$$

and

$$L_{22}^{(1)}/u_2' \approx 9.5 \times 10^{-3} \text{ sec}$$

these values being very close to Θ_{11} and Θ_{22}, respectively. The scaling factor $L_{22}^{(1)}/u_2'$ is also in good agreement with Θ_{22} in the case of the inner part of a boundary layer. In effect, from the recent measurements of Blackwelder and Kovasznay,[8] it is possible to obtain the following values:

at $x_2/\delta = 0.45$:

$$\Theta_{11} \approx 190 \times 10^{-3} \text{ sec}; \qquad L_{11}^{(1)}/u_1' \approx 210 \times 10^{-3} \text{ sec};$$

$$\Theta_{22} \approx 75 \times 10^{-3} \text{ sec}; \qquad L_{22}^{(1)}/u_2' \approx 60 \times 10^{-3} \text{ sec};$$

at $x_2/\delta = 0.20$:

$$\Theta_{22} \approx 60 \times 10^{-3} \text{ sec}; \qquad L_{22}^{1}/u_2' \approx 52 \times 10^{-3} \text{ sec}.$$

This information is of value in estimating memory times which are important features of the dynamics of turbulent flows.

[1] J. Sabot and G. Comte-Bellot, C.R. Acad. Sci. A **273**, 638 (1971).
[2] J. Sabot and G. Comte-Bellot, C.R. Acad. Sci. A **275**, 1647 (1972).
[3] J. Sabot and G. Comte-Bellot, C.R. Acad. Sci. A **275**, 667 (1972).
[4] G. Comte-Bellot and S. Corrsin, J. Fluid Mech. **48**, 273 (1971).
[5] L. S. G. Kovasznay, V. Kibens, and R. F. Blackwelder, J. Fluid Mech. **41**, 283 (1970).
[6] F. H. Champagne, V. H. Harris, and S. Corrsin, J. Fluid Mech. **41**, 81 (1970).
[7] A. Favre, J. Gaviglio, and R. Dumas, J. Fluid Mech. **3**, 344 (1958).
[8] R. F. Blackwelder and L. S. G. Kovasznay, Phys. Fluids **15**, 1545 (1972).
[9] V. H. Harris and S. Corrsin, Bull. Am. Phys. Soc. **17**, 1089 (1972).